

Polarized Beams From  $\Sigma^+$  Decay

David C. Carey

Fermi National Accelerator Laboratory

Batavia, Illinois 60510

I. Background

The existing polarized proton beam at Fermilab produces polarized protons by the decay of lambda hyperons. Since the lambda particles are neutral, no momentum selection is possible. Momentum selection is done entirely on the decay products, the polarized protons. The direction of polarization of the proton is correlated with the direction of the proton momentum in the lambda center of mass. The direction of the momentum can be correlated with the transverse position of the protons at an intermediate focus in the beam line. The transverse polarization is identified at this point, and positive and negative horizontal transversely polarized particles are transmitted through the beam line simultaneously.

In the fall of 1987, Rafil Rzaev, a visitor to Fermilab from Serpukhov, proposed an alternate targetting scheme. He suggested that polarized protons be produced by positive sigma hyperons. Momentum selection could then be done on both the parent particles and the decay products (the protons). The resultant protons would be polarized longitudinally.

At the end of his brief stay, he asked to use my computer program to verify the feasibility of his scheme. The idea for this alternate arrangement is then entirely his. I have filled out some details and made some comparisons which I shall describe below.

## II. Targetting Scheme for $\Sigma^+$

The targetting scheme for  $\Sigma^+$  is shown in figure 1. The primary proton beam is displaced transversely from its normal position by upstream bending magnets. Immediately before the target it is bent 12 mr toward the polarized proton beam axis. The subsequent bending magnets shown are used as sweeping magnets when polarized protons are produced from lambda hyperons. Here they are set to bend 310 GeV positive particles onto the axis of the polarized proton beam. The 800 GeV incident protons are bent only 4.2 mr, and thus diverge from the polarized beam axis by 7.8 mr. They are thereby directed toward a beam dump.

The  $\Sigma^+$  particles decay rapidly in the early part of the polarized beam. For comparison we have listed the characteristics of the  $\Lambda$  and  $\Sigma^+$  particles in table 1. The masses are comparable but the  $\Sigma^+$  decays about three times as rapidly as the  $\Lambda$ . The decay constant is given in nanoseconds, meters per GeV/c, and meters at 200 GeV/c. Because of the rapid decay of the  $\Sigma^+$  particles, essentially all polarized protons are produced before the  $\Sigma^+$  particles reach the first optical element of the polarized proton beam. The distribution of decay positions at 200 GeV/c for  $\Lambda$  and  $\Sigma^+$  hyperons, along with the position of the downstream end of the sweeping magnet are shown in figure 2.

	$\underline{\Lambda}$	$\underline{\Sigma}^+$
charge	0	+
mass (GeV/c <sup>2</sup> )	1.11560	1.18937
lifetime (ns)	26	8
m/GeV/c	.0707	.0202
m @ 200 GeV/c	14.1	4.0
Decay Modes	$p\pi^-$ (64.2%)	$p\pi^0$ (51.6%)
	$n\pi^0$ (35.8%)	$n\pi^+$ (48.4%)
Polarization parameter $a$	.647	-.979
$\langle P \rangle = a\hat{k}$		

Table I. Particle Characteristics

The disadvantage of the rapid decay is that a large fraction of the  $\Sigma^+$  particles decay in the sweeping magnet. The flux estimates given in this paper were made using the 13.5 kilogauss sweeping magnet presently in the polarized proton facility. However, 35 kilogauss fields have been achieved in the Fermilab charged hyperon facility. Using a shorter higher-field magnet in the  $\Sigma^+$  beam will considerably enhance the flux of polarized protons. The field quality is not terribly important for two reasons. (1) The sweeping magnet is close to the target and field errors will mostly change the effective production angle of the  $\Sigma^+$  hyperons. (2) The change in particle direction from the decay will broaden the image in the polarized proton beam more than will the sweeping magnet field errors.

The polarized proton beam is tuned to a momentum of 200 GeV/c and is unchanged from its use with  $\Lambda$  hyperons. The mismatch in momentum between the  $\Sigma$  hyperons and the protons limits the beam transmission to positive particles produced by the decay of positively charged parent particles. No particles of any momentum, directly produced at the target can reach the end of the polarized proton channel.

The protons resulting from the  $\Sigma^+$  decay have a momentum which ranges from 65 to 96 percent of the  $\Sigma^+$  momentum. For a given momentum  $\Sigma^+$ , the distribution of protons is uniform in this momentum range. The most forward produced particles have the highest momentum and would form the best final beam spot. However, tuning for this maximum momentum would allow directly produced particles through the polarized proton channel. The design described here has a proton momentum fraction of 65 percent. The flux from a competing background particle production process will depend on its decay momentum fraction range as well as on the usual factors of parent production cross section and branching ratio.

The branching ratio of  $\Lambda$  into protons is slightly higher than that of  $\Sigma^+$  into protons. However, these two branching ratios differ by a factor which is no larger than are the uncertainties in flux estimates. Detailed descriptions of flux estimates will be given below.

One of the big advantages in using  $\Sigma^+$  hyperons to produce polarized protons is that the correlation of polarization with decay direction is greater than it is for  $\Lambda$  decay. Protons produced by backward or forward decay will be longitudinally polarized. Selection of a momentum fraction of 65 percent produces backward polarized protons. If the momenta of both the  $\Sigma^+$  and the proton could be chosen exactly, a 98 percent polarized proton beam could be produced. Flux considerations require a broader banded acceptance and thus lower the net final polarization.

The longitudinal polarization contrasts with the transverse polarization of the polarized proton beam produced by  $\Lambda$  hyperons. However, the use of the Siberian snake at the end of the beam line allows the transformation of any direction of polarization into any other direction. The two transverse polarization modes can then be alternated by reversing the fields of the snake magnets. Any systematic effects associated with asymmetric beam line acceptances will thereby be reduced.

### III. The Resulting Beam

For comparison we begin with a description of the characteristics of the existing beam. The polarization of the protons at the final focus is strongly correlated with horizontal position at the intermediate focus. The polarization is then determined by means of tagging hodoscopes at this intermediate focus.

In figure 3 is shown the transverse distribution of particle intensity at this intermediate focus. Also shown is the average polarization as a function of horizontal position at this intermediate focus. The polarization seems to level out to a maximum magnitude of 50 percent when the particles are at least 8 mm from the beam center line. However, this region is also the tail of the intensity distribution and represents only about 10 percent of the total flux. The maximally polarized flux is then only 10 percent of the flux of the beam line.

In the  $\Sigma^+$  produced polarized proton beam there is no correlation of polarization with any transverse position and hence no tagging. The protons are longitudinally polarized. The average polarization was calculated to be 63 percent. The flux is approximately 10 percent of the proton flux for the  $\Lambda$  produced beam. This means that the maximally polarized flux is close to being equal for the two different beam lines.

The original calculations for the new targetting scheme were done using the existing  $\Lambda$  production model for the  $\Sigma^+$ . More accurate calculations required a determination of the comparative production rates of the two particles. Data for the  $\Lambda$  production rate from 400 GeV protons was directly available. That for  $\Sigma^+$  production was expressed as a ratio of various kinds of hyperons to pions. The pion production rate was estimated by scaling results from production by 200 GeV protons. From this comparison it was determined that no improvement could be made on the use of the  $\Lambda$  parameterization to approximate the  $\Sigma^+$  production. References are given below.

Polarized protons are not the only particles which emerge from the beam line. A variety of background processes produce other particles. The major processes are given in table II. The fluxes given are for  $3 \cdot 10^{12}$  800 GeV protons incident on a half interaction length target. In other words, there are  $1.2 \cdot 10^{12}$  interacting protons.

The momentum fraction for each decay process is also given. This fractional range, when multiplied by the momentum of the parent particle, gives the momentum range of the progeny particle. As mentioned above, the limits of this range can strongly influence the flux that is transmitted by the beam line. If the range is low, as for  $\pi^+$  produced by  $\Sigma^+$ , then higher momentum parents are required to produce the progeny particles. The parent production flux and hence the progeny flux is lower at this higher energy.

The flux for  $\Lambda$  producing polarized protons is also given. As mentioned above, only about 10 percent of this flux as close to 50 percent polarization. This means that the useful polarized proton fluxes from  $\Lambda$  and  $\Sigma^+$  decay are comparable.

	<u>Momentum Fraction</u>	<u>Rate</u>
$\Sigma^+ \rightarrow p$	65 - 96 %	$2.7 \cdot 10^6$
$\Sigma^+ \rightarrow \pi^+$	4 - 35 %	$1.2 \cdot 10^5$
$p, \pi^+$ direct	100 %	0
$K^+ \rightarrow \pi^+$	9 - 92 %	$8 \cdot 10^4$
$\pi^+ \rightarrow \mu^+$	57 - 100 %	$4.4 \cdot 10^6$
$K^+ \rightarrow \mu^+$	4 - 100 %	0
$\Lambda \rightarrow p$		$3.1 \cdot 10^7$

$3 \cdot 10^{12}$  protons incident on 1/2 interaction length target

( $1.2 \cdot 10^{12}$  interacting protons)

Table II. Competing Processes

Horizontal and vertical beam profiles at the final focus are shown in figure 4. The rms full width of the beam is about 1 cm in both transverse planes. The more rapid decay of the  $\Sigma^+$  compared to the  $\Lambda$  helps reduce the final spot size. The virtual transverse displacement at the beginning of the beam is equal to the angle between the hyperon and proton trajectories times the distance from the start of the beam to the point of decay. The average value of the latter is smaller for more rapid decay. The virtual source size and therefore the final spot size are then smaller.

References

- A.E. Brenner et al, Experimental Study of Single-Particle Inclusive Hadron Scattering and Associated Multiplicities, Physical Review D 26, 1497 (1982).
- T.R. Cardello et al, Charged-Hyperon Production by 400-GeV Protons, Physical Review 32, 1 (1985).
- J. Lach and L. Pondrom, Hyperon Beam Physics, Annual Review of Nuclear and Particle Science 29, 203 (1979).
- Pondrom, Lee G., Hyperon Experiments at Fermilab, Physics Reports 122, 58 (1985).



Figure Captions

Figure 1. The targetting scheme for  $\Sigma^+$ . The 800 GeV/c primary proton beam enters from the left parallel to the axis of the polarized proton beam. It is deflected 12 mr toward the production target. The  $\Sigma^+$  decay in the two sweeping magnets into polarized protons which are transmitted by the polarized proton beam line. The primary protons which remain are deflected only 4.2 mr into the beam dump.

Figure 2. The distribution of decay positions at 200 GeV/c for  $\Lambda$  and  $\Sigma^+$  hyperons. Also shown is the downstream end of the sweeping magnets.

Figure 3. The transverse distribution of particle intensity at the intermediate focus. Also shown is the average polarization as a function of horizontal position at this intermediate focus.

Figure 4. Beam profiles at the final focus in the horizontal and vertical planes.

# TARGETTING SCHEME FOR $\Sigma^+$

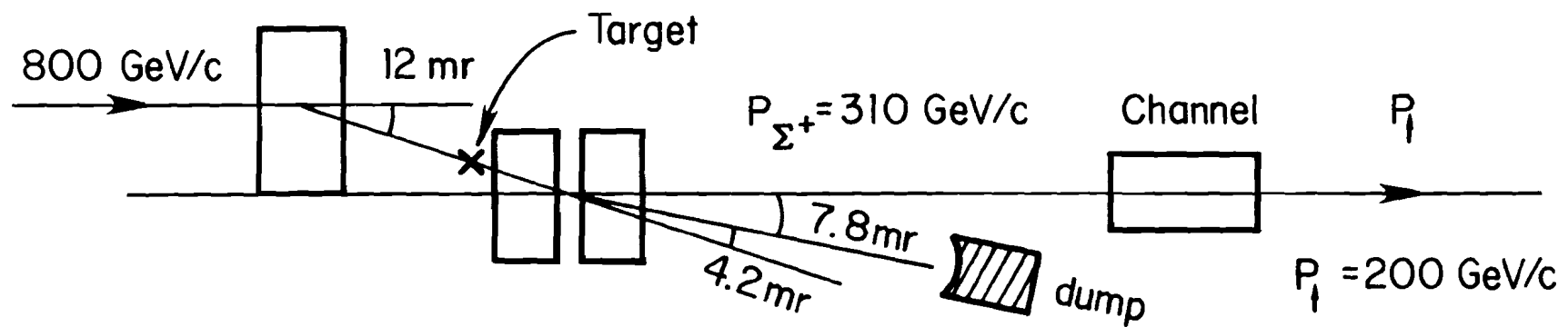


Fig. 1

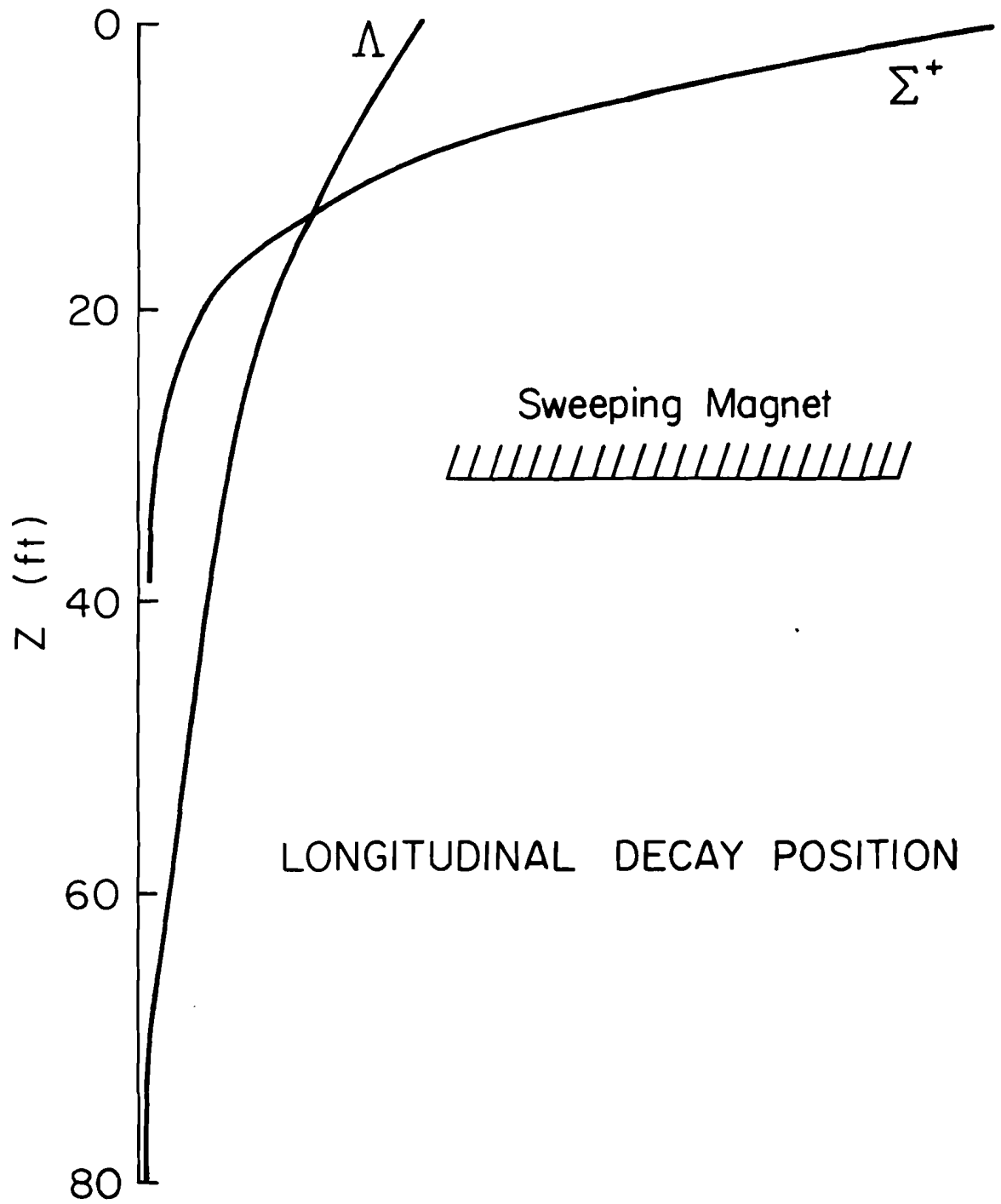


Fig. 2

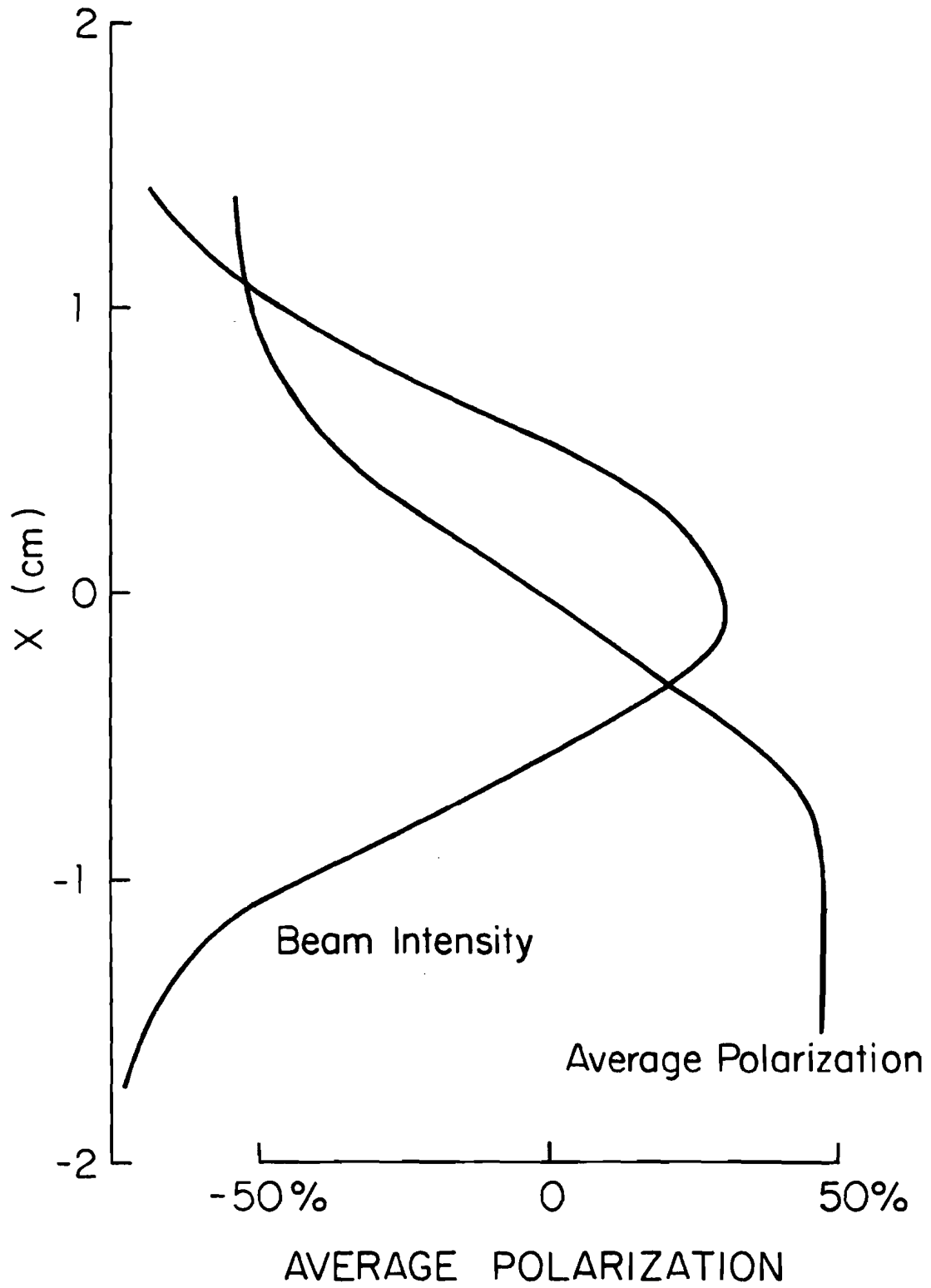


Fig. 3

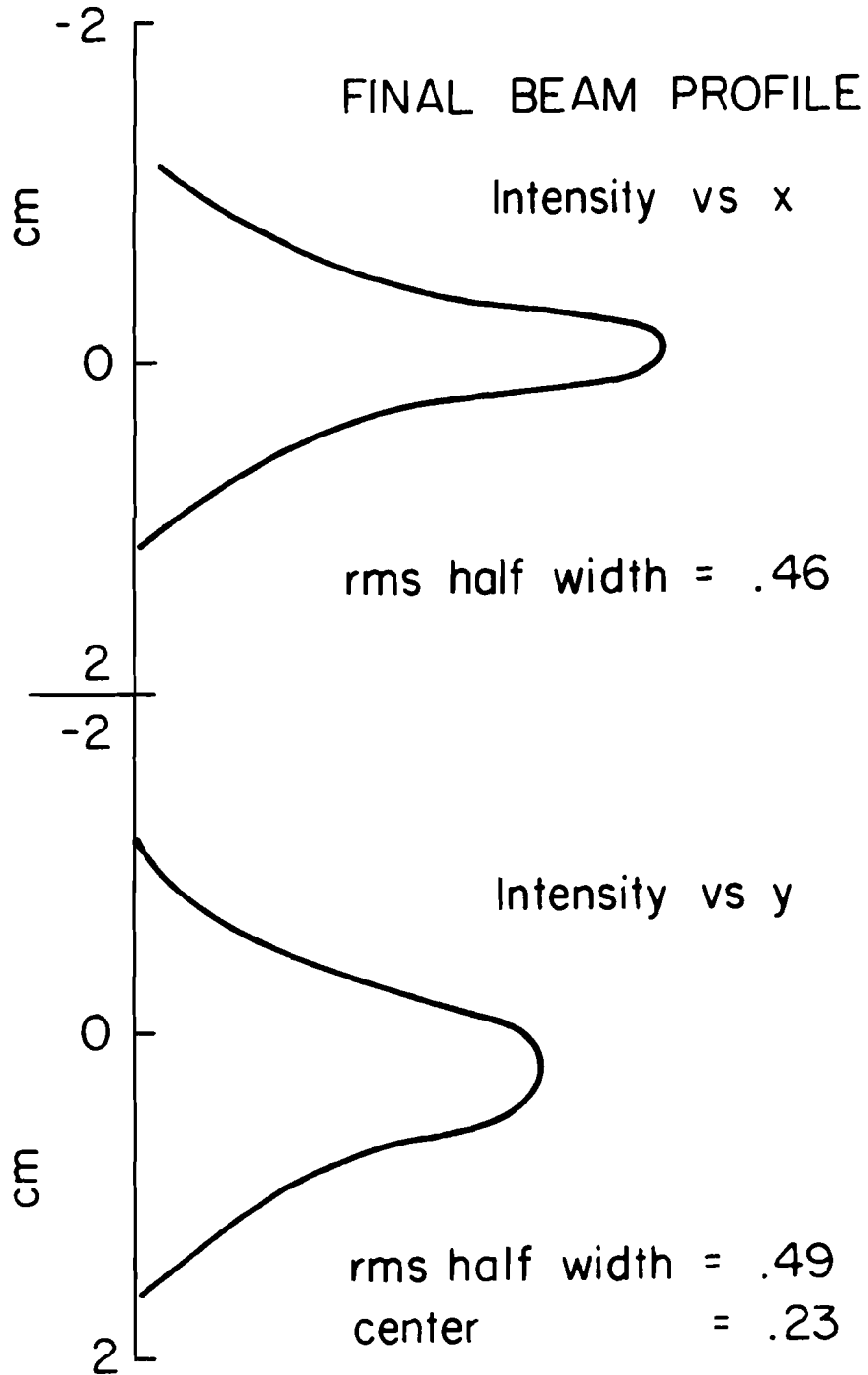


Fig. 4

